

Electronic Supplementary Information (ESI)

**Low-temperature selective catalytic reduction of NO with
NH₃ over nanoflaky MnO_x on carbon nanotubes *in-situ*
prepared via a chemical bath deposition route**

Cheng Fang,^{a,b} Dengsong Zhang,^{*a,b} Sixiang Cai,^b Lei Zhang,^b Lei Huang,^b Hongrui Li,^b

Phornphimon Maitarad,^b Liyi Shi,^{b,c} Ruihua Gao^b and Jianping Zhang^{b,c}

^a School of Material Science and Engineering, Shanghai University, Shanghai 200072, China. Fax: 86 21 66136079; E-mail: dszhang@shu.edu.cn

^b Research Center of Nano Science and Technology, Shanghai University, Shanghai 200444, China.

^c Department of Chemistry, Shanghai University, Shanghai 200444, China. E-mail: shiliyi@shu.edu.cn

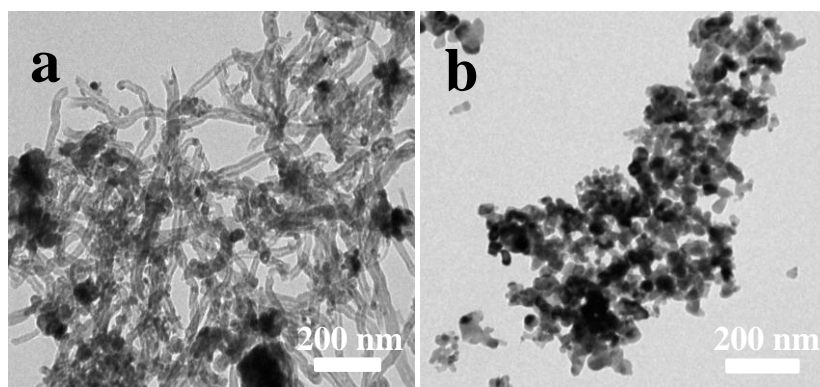


Fig. S1. TEM images of (a) MnO_x/CNTs and (b) MnO_x/TiO₂.

Fig. S1 shows the TEM micrographs of MnO_x/CNTs and MnO_x/TiO₂. Obvious aggregated particles can be observed on the surface of CNTs for MnO_x/CNTs in Fig. S1(a). Similarly, the manganese oxides and TiO₂ nanoparticles mix together and a large number of aggregates are formed as shown in Fig. S1(b).

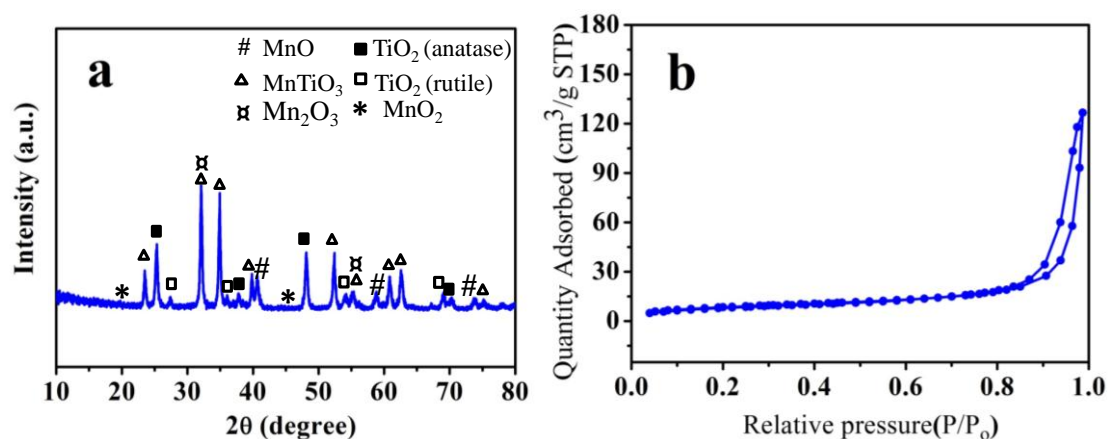


Fig. S2. (a) XRD pattern and (b) N₂ adsorption-desorption isotherms of the MnO_x/TiO₂.

The XRD pattern of MnO_x/TiO₂ was shown in Fig. S2(a), there were two phases of TiO₂. Besides the anatase phase, several weak peaks were apparently assigned to rutile TiO₂. Clearly, the manganese oxides existed mainly as MnTiO₃ (JCPDS 29-0902) in the catalyst, illustrating a strong interaction between TiO₂ and manganese.¹ Besides, although several small peaks were apparent for crystalline MnO, Mn₂O₃ and MnO₂, the intensity of these bands was very low, indicating the low content of these oxides. The N₂ adsorption-desorption isotherms of the MnO_x/TiO₂ catalyst are presented in Fig. S2(b). The shape of the adsorption isotherms and hysteresis loops keeps the same with other two catalysts but the nitrogen uptake occurs at higher relative pressures, displaying additional macroporosity which might be resulted from the agglomerated particles.² The BET surface area and the pore volume are calculated to be 31.3 m²·g⁻¹ and 0.18 cm³·g⁻¹, which are both smaller than those of other two catalysts.

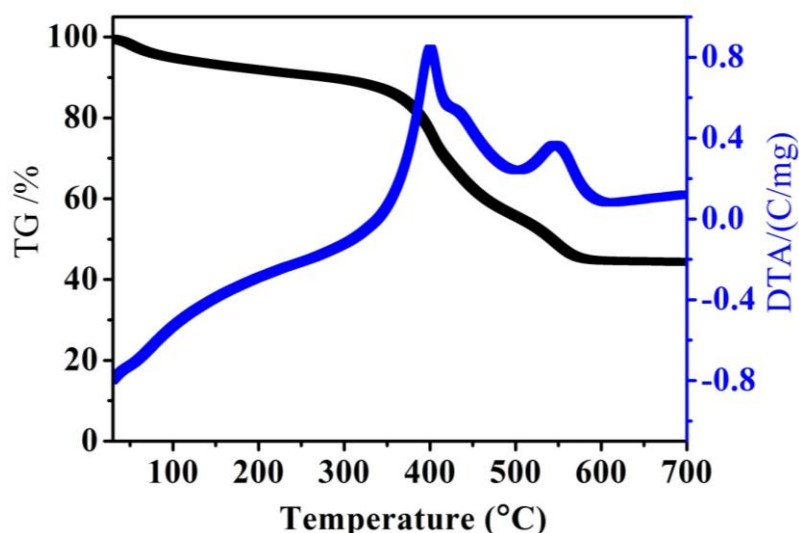


Fig. S3. TG-DTA curves of the nf-MnO₂@CNTs.

Thermal decomposition of the solid was studied by thermogravimetry and differential thermal analysis (TG-DTA) using an SDT Q600 TA instrument at a heating rate of 10 °C·min⁻¹ from room temperature to 700 °C. The TG-DTA curves of the nf-MnO₂@CNTs are presented in Fig. S3. The weight loss below 300 °C is mainly due to the elimination of water absorbed on the surface of the nf-MnO₂@CNTs composites. A sharp weight loss took place from 300 °C to 480 °C and this weightlessness may be ascribed to the phase change of birnessite-type MnO₂ and the increasing decomposition of CNTs.³ The weight loss above 480 °C might also due to the continuous phase change of manganese oxides.

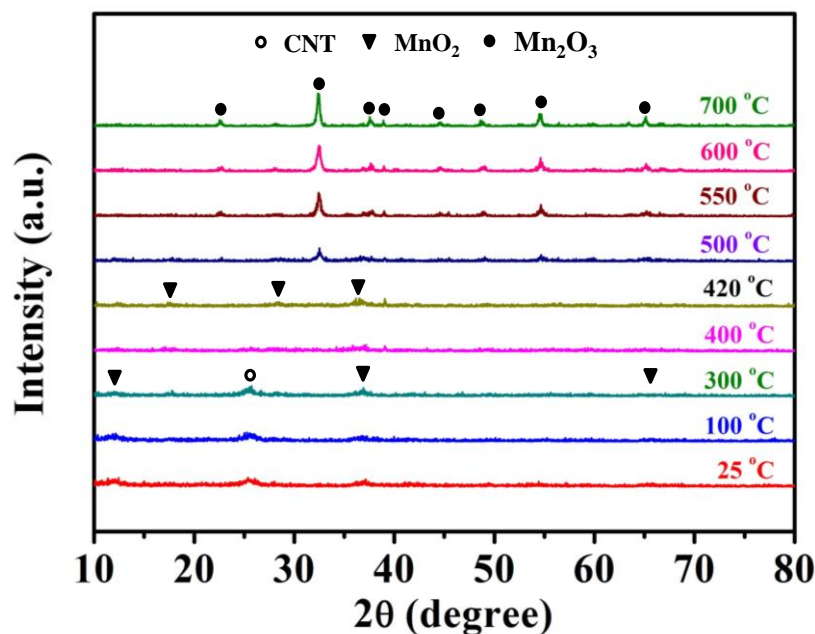


Fig. S4. *In-situ* time-resolved XRD patterns of the nf-MnO₂@CNTs.

The *in-situ* time-resolved XRD patterns (XRD) was performed with a Rigaku D/MAX-2200 X-ray diffractometer by using Cu K α (50 kV, 40 mA) radiation and a secondary beam graphite monochromator. The *in situ* time-resolved XRD patterns were performed to study the structure change of nf-MnO_x@CNTs during the hyperthermic treatment. In Fig. S4, the XRD patterns of the catalyst at temperatures below 300 °C are consistent with Fig. 3. When further increasing temperature, the diffraction peaks of CNTs began to weaken and finally faded away. Meanwhile, the diffraction patterns corresponding to birnessite-type MnO₂ receded and could not be observed at 500 °C. When the catalyst was at 420 °C, new distinct phase of MnO₂ can be clearly observed. Further raising the temperature, different diffraction peaks corresponding to Mn₂O₃ showed up, indicating the crystalline phase change of manganese species, which could explain the decreased activity of nf-MnO_x@CNTs.

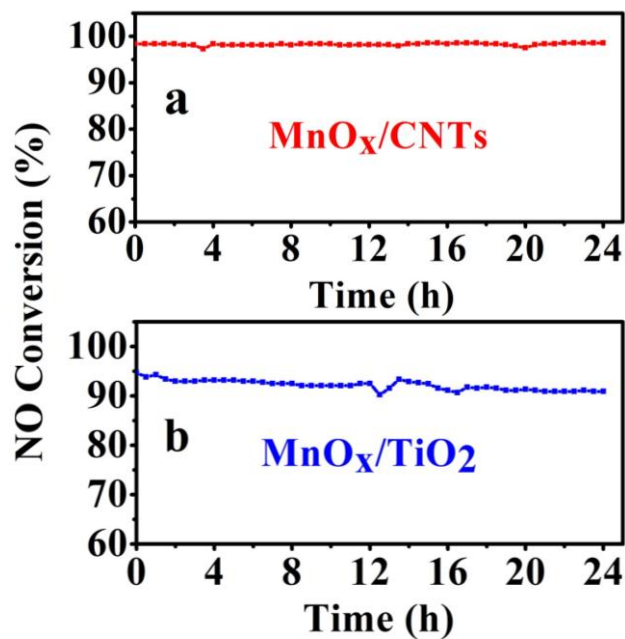


Fig. S5. Stability test of the catalysts at 225 °C. Reaction conditions: [NO] = [NH₃] = 500 ppm, [O₂] = 3 vol. %, N₂ balance, and GHSV = 30,000 h⁻¹.

Fig. S5 shows the stability tests of MnO_x/CNTs and MnO_x/TiO₂ as a function of the time at a typical temperature 225 °C. The NO conversion of MnO_x/CNTs was maintained at ca. 99.0 % during the test period. However, the activity of the MnO_x/TiO₂ was decreased within the same testing time.

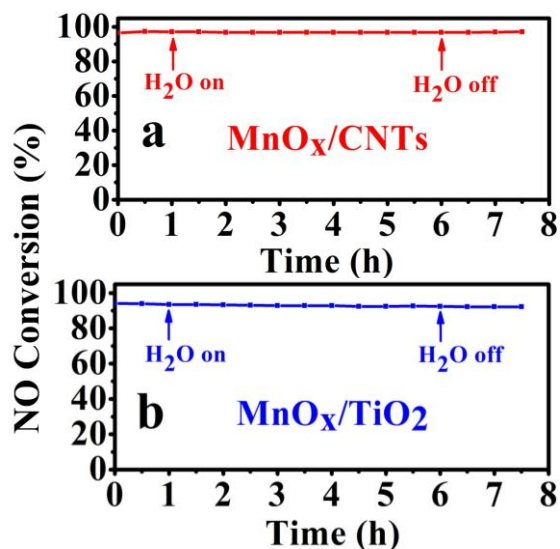


Fig. S6. H₂O resistance study of the catalysts at 225 °C. Reaction conditions: 225 °C, [NO] = [NH₃] = 500 ppm, [O₂] = 3 vol. %, [H₂O] = 4 vol. %, N₂ balance, and GHSV = 30,000 h⁻¹.

The influence of the H₂O on the SCR activity over MnO_x/CNTs and MnO_x/TiO₂ as a function of time at 225 °C was investigated and shown in Fig. S6. For MnO_x/CNTs, the activity remained unchanged during the test no matter with or without the presence of H₂O. In Fig. S6(b), when H₂O was added to the reaction gas, the slight decrease was found and the NO conversion also kept at about 92.5 % over MnO_x/TiO₂ after the H₂O supply was stopped.

References

1. K. H. Park, S. M. Lee, S. S. Kim, D. W. Kwon and S. C. Hong, *Catal Lett*, 2013, **143**, 246-253.
2. A. Szegedi, M. Popova and C. Minchev, *J Mater Sci*, 2009, **44**, 6710-6716.
3. D. S. Zhang, H. X. Fu, L. Y. Shi, J. H. Fang and Q. Li, *J Solid State Chem*, 2007, **180**, 654-660.